AOT-Microemulsions-Based Formation and Evolution of $PbWO_4$ Crystals

Di Chen, Guozhen Shen, Kaibin Tang,* Zhenhua Liang, and Huagui Zheng

Nanomaterial and Nanochemistry, Hefei National Laboratory for Physical Sciences at Microscale, University of Science and Technology of China, Hefei, 230026, P.R. China

Received: December 9, 2003; In Final Form: June 3, 2004

Anionic surfactant-AOT-microemulsions-assisted formation and evolution of $PbWO_4$ nanostructures with bundles rodlike, ellipsoidlike, and spherelike prepared at different media conditions were studied by powder X-ray diffraction pattern, field emission scanning electron microscopy, and transmission electron microscopy. The possible mechanisms for the formation of $PbWO_4$ samples in series of microemulsion systems were discussed. Various comparison experiments show that several experimental parameters, such as the AOT concentration, the water content, and reaction temperature play important roles in the morphological control of $PbWO_4$ nanostructures. Room-temperature photoluminescence of $PbWO_4$ samples with different morphologies has also been investigated and the results reveal that all these samples showed similar features with emissions at 480 ∼ 510 nm but different luminescence intensity.

Introduction

In recent years, the surfactant-assisted synthesis of nano-, microstructured inorganic materials has attracted considerable attention for its soft template effect, reproducibility, and simple maneuverability.[1,2] There are several methods based on the soft template effect that mimic the essential functions of biological membranes, for example, self-assembled monolayers, Langmuir−Blodgett (LB) films, multilayers, polymeric membranes, and reverse micelles or microemulsions.[3] The last one, reverse micelles or microemulsions, has already been verified as an effective approach to synthesize ultrafine inorganic particles.[4−10] It is well-known that certain surfactant molecules such as ionic surfactant AOT (sodium bis (2- ethylhexyl) sulfosuccinate) or nonionic surfactants, dissolved in organic solvents, are capable of solubilizing water in the polar core, and these entities are called reverse micelles or microemulsions. Accordingly, reverse micelles and microemulsions that are thermodynamically stable systems and heterogeneous on a molecular scale have the ability to solubilize macromolecules. As the organized media, they have been widely used as spatially constrained microreactors for the growth of nano- and microcrystallites with a desired narrow size distribution.[2,3] Unfortunately, in most cases only spherical particles are prepared within the polar cores of microemulsions. Traditionally, there has been a report on the successfully synthesis of microporous zincophosphate sodalite with a cubic morphology in microemulsions, which indicated that the microemulsions-based approach can not only be used as a synthetic approach, but also provides the means of controlling the morphology as well as the size of grown crystals.[11,12] Since then, various of 1-D nanoscale materials including CdS,[13] $CaSO_4$,[14] $BaWO_4$,[15] and $BaCrO_4$[16,17] have been successfully prepared in microemulsion media. All these studies suggest that the microemulsion system can be used not only as a dynamical system for the synthesis of inorganic materials through a simple and facile solution process, but to control the size and shape of inorganic particles.

As an important inorganic scintillating crystal, lead tungstate crystal ($PbWO_4$) with a stolzite structure has been the current focus of much attention. Compared to other well-known scintillators, such as BaF_2, CeF_3 and undoped CsI,[18,19] $PbWO_4$ crystal is most attractive for its high-energy physics applications because of its high density (8.28 g/cm^3), short radiation length ($X_0 = 0.92$), fast decay time($\leq$10 ns) and excellent time and energy resolution.[20,21] $PbWO_4$ crystal has been investigated since the 1940s, but was studied as a heavy scintillator for high-energy physics only in the beginning of the 1990s due to the fact that the $PbWO_4$ scintillator was successfully chosen as a scintillating medium for electromagnetic (EM) colorimeters for the Compact Muon Solenoid (CMS) experiment at the Large Hadron Collider (LHC) by the Center of Europe for Research Nuclear (CERN).[22,23] Recently, $PbWO_4$ scintillator has become the most attractive candidate to build or upgrade several small setups for the intermediate energy region, where fast response and good energy resolution are required.[20] As a matter of fact, the rare-earth element doped $PbWO_4$ has already been found to exhibit ion conductivity.[24,25] Previous studies have shown that $PbWO_4$ can be synthesized by several different techniques, such as a high-temperature solid-state reaction for powder,[26] a flux method for whisker growth,[27] the Bridgman method for single crystals,[28] and so on. These techniques are technically demanding, as they require comparatively complex procedures to achieve ultrafine products.

In the present work, we report on the synthesis of $PbWO_4$ nanostructures in a simple anionic microemulsion system. Studies found that some related experimental parameters including the concentration of the anionic surfactant, the water content, and reaction temperature have great influences on the product morphology. By carefully controlling these experimental parameters, $PbWO_4$ nanostructures with morphologies of bundles of rods, ellipsoids, spheres, dipyramids, and nanoparticles can be efficiently achieved, respectively.

Experimental Section

The anionic surfactant AOT (sodium bis (2- ethylhexyl) sulfosuccinate) was purchased from Shanghai Chemical Co. Ltd.

* Corresponding author. E-mail address: kbtang@ustc.edu.cn (K. B. Tang). Tel and Fax: (86)-551-3601791.

10.1021/jp0377681 CCC: $27.50 © 2004 American Chemical Society
Published on Web 07/09/2004

and used without further purification. Pb $(AC)_2$, ethylene glycol (EG), and $Na_2WO_4 \cdot 2H_2O$ were of A. R. grade, and the water used in this work was distilled and deionized.

The preparation of $PbWO_4$ nanostructures with various morphologies, such as sphere-, ellipsoid-, dipyramid- and rodlike in the mild AOT-contained microemulsion system is described as follows. Briefly, two separated AOT/EG/H_2O microemulsion systems containing equivalent amounts of Pb^{2+} or WO_4^{2-} (0.66 M), respectively, were mixed after mechanical agitation for about 20 min. The solution became obviously turbid quickly, indicating the formation of the $PbWO_4$ nucleus. Then, the white precipitates were left to stand motionlessly in their mother solutions for 24 h to ensure complete equilibration. To get products with different morphologies and particle sizes, several parameters, such as the concentration of surfactant AOT, the volume ratio of water to EG solution, and reaction temperature were well controlled. After the reaction was completed, the as-obtained products were washed several times with absolute ethanol and distilled water and dried in a vacuum at 50 °C.

X-ray powder diffraction (XRD) patterns were collected on a Philips X′pert Pro Super X-ray diffractometer with Cu Kα radiation ($\lambda = 1.5418$ Å). The morphology and size of as-prepared products were observed by transmission electron microscopy (TEM), carried out on a Hitachi H-800 transmission electron microscope. Field-emission scanning electron microscope (FE-SEM) measurement was carried out with a field-emission microscope (JEOL, 7500B) operated at an acceleration voltage of 10 kV. PL emission spectra of the as-prepared samples with different morphologies were measured using a 300-nm excitation line at room temperature.

Results

The morphologies of the synthesized products were examined by field-emission scanning electron microscopy (FE-SEM). A typical FE-SEM image of the product prepared in the microemulsion system of 2 mmol AOT and 30 mL EG at room temperature (Figure 1a) shows that the product consists of a large quantity of bundles of $PbWO_4$ nanorods. The typical length of the bundle is about 3.5 ∼ 4.5 μm. A high magnification FE-SEM image (Figure 1b) shows that each bundle is actually formed by lots of $PbWO_4$ nanorods branched out radically from the revolutional axis of the rod bundles in a uniform size-distribution. The average diameter of a single $PbWO_4$ nanorod is about 45 nm and the length of the axis is up to 3.5 μm. The SAED pattern (inset in Figure 1b), taken from a randomly chosen single rod, shows that it is well crystallized but exhibits dot elongation, which may be caused by the other $PbWO_4$ nanorods in the bundle with an oriented crystallographic axis. Interestingly, when the reaction was performed at the higher temperature of 40 °C, FE-SEM images showed that the products are composed of almost monodispersed ellipsoidlike nanostructures with uniform grain sizes (Figures 1c and 1d). The length of the minor axis of the ellipsoids is about 350 ∼ 550 nm and that of the major axis in the range of 1 ∼ 1.5 μm. Figures 1e and 1f show the FE-SEM images of the product obtained in another microemulsion system, which contains 2 mmol AOT, 25.5 mL EG, and 4.5 mL H_2O at room temperature. It clearly shows that the products are microspheres with uniform size distribution, which are homogeneously distributed on the copper slide. By carefully controlling the distribution, these spheres can form one or two layer structures, which may find potential application in nanodevices. The detailed results of the above analyses are listed in Table 1.

The phase composition and phase structure of as-obtained products were examined by powder X-ray diffraction (XRD).

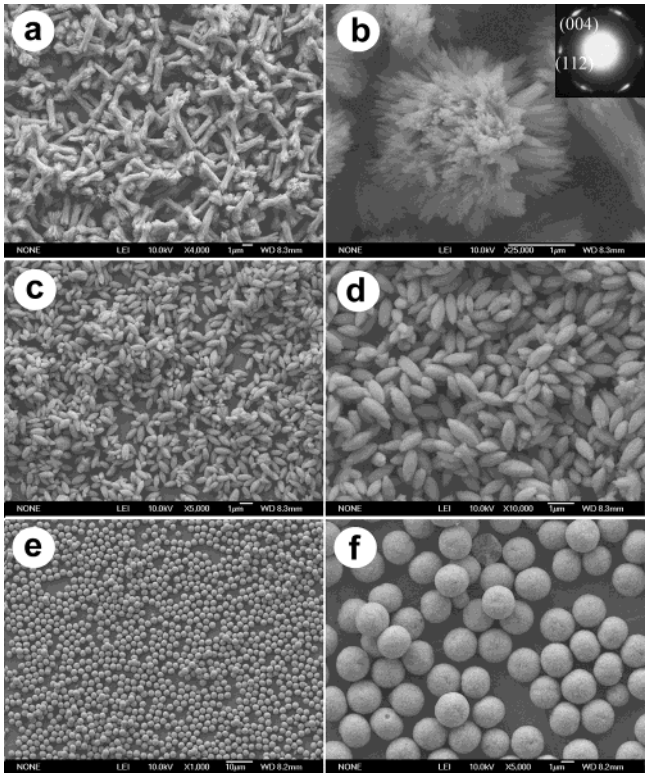

Figure 1. FE-SEM images of the final products: (a, c, e) Low-magnification images of rodlike bundles, ellipsoidlike, and spherelike crystals, respectively: (b, d, f) High-magnification images of rodlike bundles, ellipsoidlike, and spherelike crystals, respectively; SAED pattern of a single rod is inset in Figure 1b.

TABLE 1: Products with Typical Morphologies and Reaction Conditions for $t = 24$ h

sample no.	reaction media	reaction temp. (°C)	morphology
S1	AOT (2 mmol)/EG (30 mL)	∼25	bundles of rods
S2	AOT (2 mmol)/EG (30 mL)	40	ellipsoids
S3	AOT(2 mmol)/EG(25.5 mL)/ H_2O(4.5 mL)	∼25	spheres

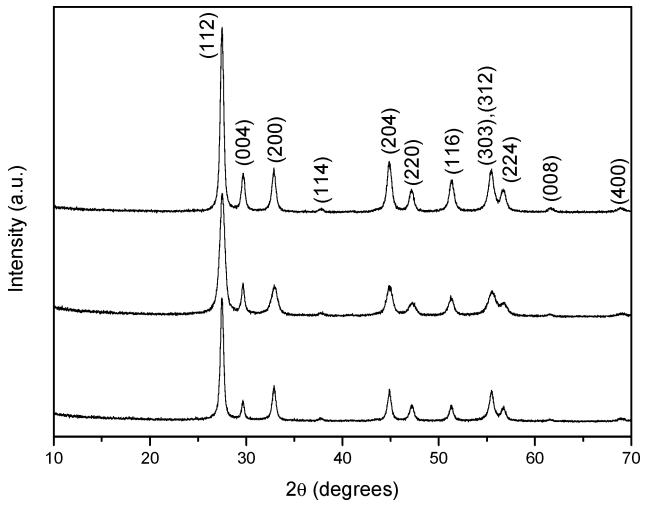

Figure 2. XRD patterns of (a) ellipsoidlike; (b) rodlike bundles; (c) spherelike.

Figure 2 shows the XRD patterns of as-obtained $PbWO_4$ samples (a, b, and c are that of the corresponding rodlike bundles, ellipsoidlike, and spherelike product, respectively). On each pattern, all the strong peaks can be well assigned to the tetragonal phase $PbWO_4$ ($a = 5.41$ Å, $c = 12.04$ Å) reported

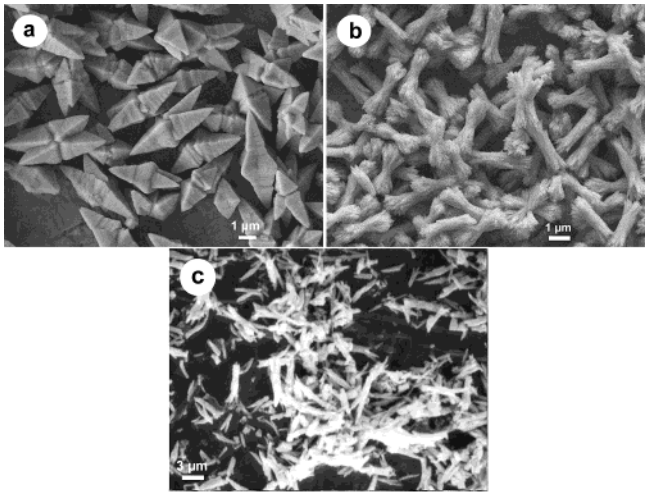

Figure 3. FE-SEM images of the products under different AOT concentrations: (a) 0.03. (b) 0.06, and (c) 0.16 mol/L.

TABLE 2: Varying Surfactant Concentration on Product Synthesis in Microemulsions at Room Temperature for $t = 24$ h

AOT/mol·L^{-1}	structure composition
0.03	dipyramids
0.06	bundles of rods
0.16	nanorods

in the literature (JCPDS card No 85-1857), and no peaks of other impurities were detected.

Discussion

Effect of AOT Concentration. In the present work, it is found that the concentration of surfactant AOT has great influence on the morphologies of the obtained samples. Figure 3 presents SEM images of $PbWO_4$ nanostructures with different morphologies including dipyramids, bundles of nanorods, and individual nanorods obtained in the AOT/EG microemulsion system by only varying the AOT concentration. The results are summarized in Table 2. We have shown that uniform bundles of $PbWO_4$ nanorods formed when the concentration of AOT was 0.06 mol/L (Figure 3a and Figure 1a). But, when the concentration of AOT was decreased to 0.03 mol/L, magnificent dipyramidal $PbWO_4$ nanostructures were obtained in the AOT-contained microemulsion system (Figure 3b). From this image, it is clearly shown that the samples are composed of a dipyramid shape with a typical side length of about 2 μm. Reasons for this result may lie in fewer surfactant molecules absorbed on the particle surface, low growth rate, and the unusual crystal habits of $PbWO_4$ playing an important role, resulting in the formation of the final morphology. Continuing to increase the AOT from 0.03 to 0.16 mol/L resulted in the formation of short $PbWO_4$ nanorods of about 1 $\sim$ 3 μm in length and several hundred nanometers in diameter, just as shown in Figure 3c, with some similar shapes to that of rod bundles.

Effect of Water Content. In addition to the effect of AOT on the morphologies of the products, studies also found that the water in the microemulsion system is another important influence factor. Table 3 illustrates the products with different morphologies that were obtained at room temperature by only changing the water content in the AOT microemulsions. When trace water (ca 4 vol %, coming from analytical EG and hydrated metal salts) existed in the microemulsion system, only bundles of $PbWO_4$ nanorods (just as shown in Figure 4a and the above analysis) were obtained. If 4.5 mL (15 vol %) water was added into the microemulsion system, spherical $PbWO_4$ nanostructures with uniform diameters were synthesized, as described above (Figure 4c). Controlling the water content of the AOT-contained microemulsion solution at 4 $\sim$ 15 vol %, $PbWO_4$ nanostructures with different proportion of nanorod bundles and spheres (Figure 4b) were formed at room temperature. One can estimate that at different percentages of water content, microemulsions with different microstructures are formed, which not only exhibit a considerable inhibition effect on the $PbWO_4$ crystallization but also show considerably influence on the crystal growth of $PbWO_4$. When the water content was increased to 50 vol % or above, only $PbWO_4$ nanoparticles with a mean size of ca. 20 nm were obtained; this may be caused by the collapse of microstructures of the formed microemulsions at high water percentage (Figure 4d).

TABLE 3: Products with Typical Morphologies Varying the Water Content in Microemulsions at Room Temperature for $t = 24$ h

volume % of water	structure composition
4	bundles of rods
4 $\sim$ 15	bundles of rods and spheres
15	spheres
50	nanoparticles

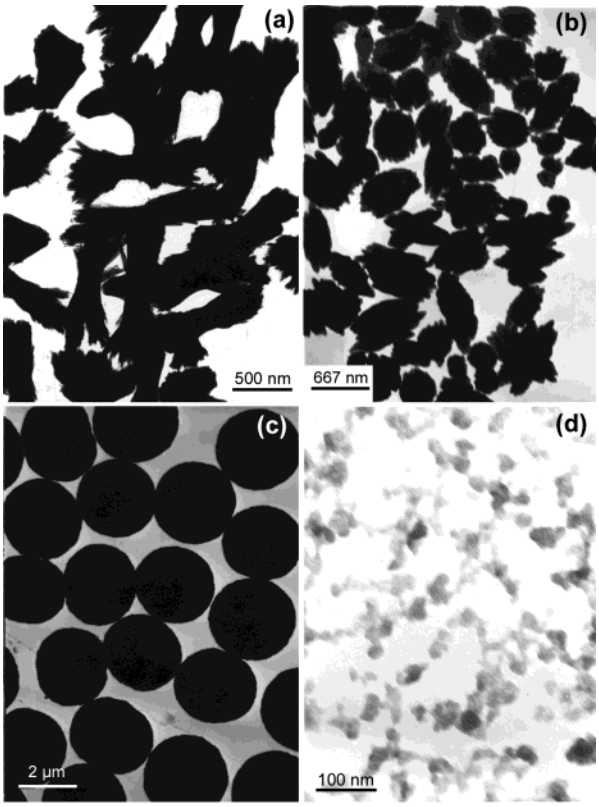

Figure 4. TEM images of the products under water content: (a) 4 vol %, (b) 10 vol %, (c) 15 vol %, and (d) 50 vol %.

Effect of Reaction Temperature. Temperature-dependent experiments for $PbWO_4$ nanostructures were also carried out and they show that reaction temperature is another important parameter that affects the morphology of as-obtained samples. The results of reaction temperature on the morphologies of the products obtained in the AOT/EG microemulsion system are shown in Table 4 and they are discussed as follows. Figure 5 shows TEM images of the samples prepared at different temperatures. At 40 °C, the TEM image shows that the

TABLE 4: Effect of Varying Reaction Temperature on Product Synthesis in Microemulsions at the Water Content of 4 Vol % for $t = 24$ h

reaction temp. (°C)	structure composition
40	ellipsoids
40 ~ 80	ellipsoids and spheres
80	spheres

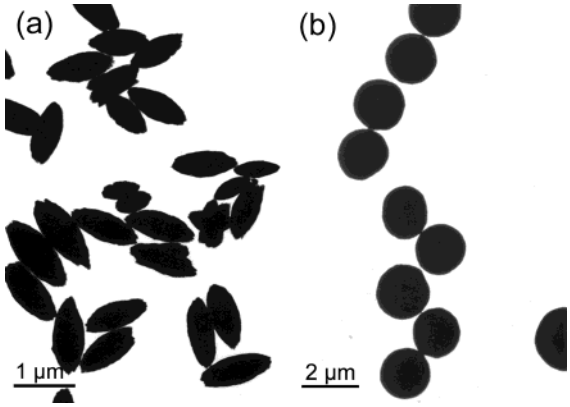

Figure 5. TEM images of the products under different reaction temperatures: (a) 40 °C and (b) 80 °C.

as-prepared samples are of ellipsoidal morphology just as shown in Figure 5a. Increasing the reaction temperature resulted in the formation of spherical $PbWO_4$ samples. When the reaction temperature rose to 80 °C, all the samples were of spherical morphology. Keeping the reaction temperature between 40 and 80 °C, the products are $PbWO_4$ with a different proportion of ellipsoids and spheres. Compared with the spherical $PbWO_4$ obtained in the AOT/EG/H_2O microemulsion system, the diameter of the spheres at 80 °C is much smaller and is about 1 μm (Figure 5b). Namely, spheres obtained at higher temperature have a smaller diameter compared to those synthesized at room temperature. Therefore, the products with different morphologies can be synthesized in the microemulsions through controlling the reaction temperature.

Possible Formation Mechanism. From the above analyses, it can be seen that the morphologies of the final products were greatly dependent on the experimental conditions, such as AOT concentration, water content, reaction temperature, and so on. According to the literature,[29,30] in the microemulsion solution AOT used as anionic surfactant is a twin-tailed surfactant and is most commonly used to make microemulsions because of its bulky hydrophobic tail to the hydrophilic group. It tends to self-assemble to form aggregates, which further lead to the formation of microemulsions with desired microstructures. This is helpful to the formation of products with some similar shapes to the microstructures of microemulsions.

In the water-in-oil microemulsions with suitable water content (4.5 mL, 15 vol %), lots of surfactant molecules selforganize to spherical droplets containing lead or tungstate ions,[29,31] respectively. All these spherical microstructures dispersing in the continuous oil media are relatively stable ahead of mixing. When the solutions dissolving equivalent [Pb^{2+}] or [WO_4^{2-}] are mixed, microemulsions with the spherelike microstructures would collide and fuse, simultaneously exchanging ions of lead or tungstate that are surrounded in the spherical microemulsion droplets but still free to move. The nucleation takes place rapidly at once, which can be satisfactorily testified because white precipitates appeared only 2 ~ 3 s after the mixing of the microemulsions. Further self-organization of the nucleus would lead to the formation of spherelike $PbWO_4$ samples through the Ostwald ripening process. However, in this case the dimensions of samples produced from the reaction are many times larger than the typical dimensions for microemulsion droplets of around 5 ~ 100 nm.[32] We conjectured that the diameters of spheres are not confined strictly by that of AOT spherelike microstructures. Due to the flexibility of the microstructure interface, $PbWO_4$ spheres will growth continually at the base of initially formed spherical microstructures. But the AOT microemulsions with very low water content (or even without water at all) cannot be described in terms of spherical microstructures; they usually selfassemble to form cylindrical- or rodlike microstructures.[30,33] Such a possible growth process has been observed by Sugimoto and co-workers[34−36] in the synthesis of peanutlike hematite ($\alpha - Fe_2O_3$) crystals with very similar shape and size from a gel−sol method in the presence of sulfate ions, where they disclosed that the bidentate-specific adsorption of sulfate ions to the growing surfaces parallel to the *c* axis resulted in the formation of hematite nanorods.[37] The mechanism for the formation of the peanutlike shape has been explained in terms of the formation of the gradual outward bending of the dense rodlike subcrystals or nanorods on both ends of ellipsoidal particles by the growth of new crystalline nanorods in the spaces between the existing subcrystals.[36] This growth process has been strongly supported by recent computer simulation results.[38] In our experiments, it can be reasonably assumed that the sulfonic acid groups of AOT could be preferentially adsorbed on the growing surfaces parallel to a certain crystallographic direction of $PbWO_4$, resulting in rodlike nanostructures. Therefore, rod bundles of $PbWO_4$ nanostructures could be formed in a way similar to the case of peanutlike hematite particles; that is, through outward bending of adjoining subcrystals by nucleation and growth of a new subcrystal in each space between them. It is noteworthy that all of the $PbWO_4$ samples obtained in the microemulsion solution exhibit nanocrystalline structure and are very likely composed of rodlike nanocrystals that act as building blocks or subcrystals. Meanwhile, the presence of a double-tailed hydrophobic group in AOT would play the role of a spacer, which is present between the growing subcrystals jostling one another and so would enhance the outward bending of the subcrystals, favoring the formation of bundles rods. Experimental observations support our assumption. After a long ultrasonic treatment on the sample, the rodlike-bundles morphology was a little damaged and many single shorter nanorods appeared. With increasing temperature, the microemulsion system under the delicate balance between the kinetic growth and thermodynamic growth regimes might be of low viscosity and instability. Cheon et al.[39] have reported that there are four different parameters, kinetic energy barrier, temperature, time, and capping molecules, that can influence the growth pattern of nanocrystals under nonequilibrium kinetic growth conditions in the solution-based approach. In this case, it is clear that the temperature and capping molecules (AOT) are the key parameters. Spherical microstructures formed because of low surface energy and high stability and further aggregated into spherical products at higher temperature. From these results, it is clearly seen that anionic surfactant AOT in the microemulsion solutions, which freely self-organize into rodlike, cylindrical-like, or spherelike microstructures under appropriate reaction conditions, were used as the soft template for the synthesis of products with unique morphologies. Due to the soft template effect, the products can duplicate the microstructures of the AOT microemulsions and grow up sequentially,. This can be identified as the AOT-microemulsions-based formation and evolution route of $PbWO_4$ nanostructures.

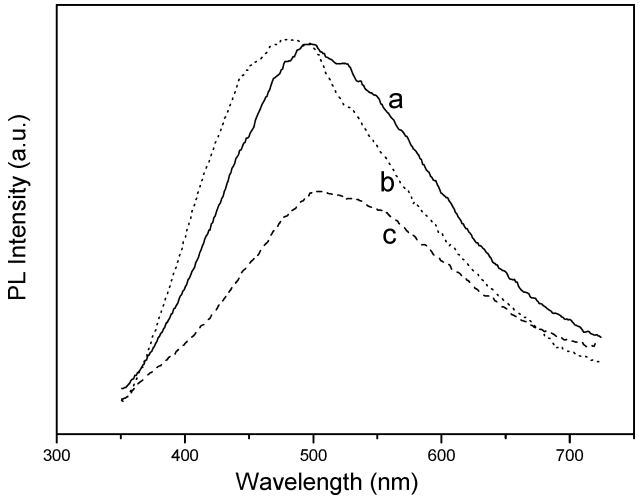

Figure 6. Room-temperature PL spectra of (a) ellipsoidlike, (b) rodlike bundles, (c) spherelike $PbWO_4$ samples.

Photoluminescence Properties. Room-temperature photoluminescence (PL) properties of the as-obtained samples were also studied. Figure 6 shows the PL spectra of the samples with ellipsoidlike, rodlike bundle, and spherelike morphologies measured using excitation line at 300 nm. The spectra show that all of the three samples exhibited green emission peaks at 480−510 nm, similar to the result reported by Shi et al.[40] The corresponding strongest PL emission peaks for ellipsoidlike, rodlike bundle, and spherelike $PbWO_4$ nanostructures appear at 498, 481, and 506 nm, respectively. Very weak size-dependent phenomena of PL properties observed indicate that the sizes of the as-prepared $PbWO_4$ nanostructures are so big that they are on the border of the quantum confinement regime. In the three products, studies found that the products with spherelike morphology show a weak luminescence, whereas rodlike samples display the strongest luminescence under the same measurement conditions. It is known that the morphologies and sizes greatly influence the luminescence properties of inorganic materials. Rodlike crystals would possess more defects due to faster 1-D crystal growth so they show more intense PL emission. A rough but universal explanation is that changes in the sizes and microstructures of products cause modification of the electronic structures, influencing the carriers excited from the valence band to the conduction band, which then relax their energy on the product surfaces leading to variations in luminescence.

Conclusion

In summary, $PbWO_4$ nanostructures with different morphologies, such as spherelike, rodlike bundles, ellipsoidlike, and dipyramidlike have been synthesized in a mild AOT/EG/H_2O microemulsion system. It is found that several experimental parameters, for example, the concentration of the anionic surfactant AOT, the water content (vol % in this paper) and reaction temperature have significant effects on the product's morphology and size-distribution. The possible mechanism of AOT-microemulsions-based formation and evolution of $PbWO_4$ nanostructures was put forward and well confirmed, with studying the product's results obtained under different reaction conditions. Photoluminescence of products with spherelike, ellipsoidlike, and bundles of rodlike shapes have also been investigated at room temperature using the same excitation line at 300 nm. The anionic surfactant AOT is well used as a soft template in the microemulsions and such an anionic surfactant microemulsion system may represent promising microstructured media for the synthesis of other inorganic materials with unique properties.

Acknowledgment. Financial support by the National Natural Science Foundation of China and the 973 Projects of China is gratefully acknowledged.

References and Notes

(1) Cizeron, J.; Pileni, M. P. *J. Phys. Chem.* **1995**, *99*, 410.
(2) Pileni, M. P. *Langmuir* **1997**, *13*, 3266.
(3) Fendler, J. H. *Chem. Rev.* **1987**, *87*, 877.
(4) Eastoe, J.; Warne, B. *Curr. Opin. Colloid. Interface Sci.* **1996**, *1*, 800.
(5) Desai, S. D.; Gordon, R. D.; Groda, A. M.; Cussler, E. L. *Curr. Opin. Colloid Interface Sci.* **1996**, *1*, 519.
(6) Fendler, J. H. *Curr. Opin. Colloid Interface Sc.* **1997**, *2*, 365.
(7) Sager, W. F. C. *Curr. Opin. Colloid Interface Sci.* **1998**, *3*, 276.
(8) Meier, W. *Curr. Opin. Colloid Interface Sci.* **1999**, *4*, 6.
(9) Atonietti, M. *Curr. Opin. Colloid Interface Sci.* **2001**, *6*, 244.
(10) Meyer, M.; Wallberg, K.; Kurihara, K.; Fendler, J. H. *J. Chem. Soc., Chem. Commun.* **1984**, *90*.
(11) Dutta, P. K.; Jakupca, M.; Reddy, K. S. N.; Salvati, L. *Nature* **1995**, *374*, 44.
(12) Reddy, K. S. N.; Salvati, L. M.; Dutta, P. K.; Abel, P. B.; Suh, K. I.; Ansari, R. R. *J. Phys. Chem.* **1996**, *100*, 9870.
(13) Simmons, B. A.; Li, S.; John, V. T.; McPherson, G. L.; Bose, A.; Zhou, W.; He, J. *Nano Lett.* **2002**, *2*, 263.
(14) Rees, G. D.; Evans-Gowing, R.; Hannond, S. J.; Robinson, B. H. *Langmuir* **1999**, *15*, 1993.
(15) Kwan, S.; Kim, F.; Akana, J.; Yang, P. *Chem. Commun.* **2001**, 447.
(16) Li, M.; Schnablegger, H.; Mann, S. *Nature* **1999**, *402*, 393.
(17) Kim, F.; Kwan, S.; Akana, J.; Yang, P. *J. Am. Chem. Soc.* **2001**, *123*, 4360.
(18) Gratta, G.; Newman, H.; Zhu, R. Y. *Annu. Rev. Nucl. Part. Sci.* **1994**, *44*, 453.
(19) Crystal Clear Collaboration; Anderson, S. et al. *Nucl. Instrum. Methods Phys. Res., Sect. A* **1993**, *332*, 373.
(20) Kobayashi, M.; Ishii, M.; Usuki, Y. *Nucl. Instrum. Methods Phys. Res., Sect. A* **1998**, *406*, 442.
(21) Hara, K.; Ishii, M.; Nikl, M.; Takano, H.; Tanaka, M.; Tanji, K.; Usuki, Y. *Nucl. Instrum. Methods Phys. Res., Sect. A* **1998**, *414*, 325.
(22) *Compact Muon Solenoid Technical Proposal*; CERRN/LHCC 94−38; LHCC/PI, 1994.
(23) Nikl, M.; Nitsch, K.; Hybler, J.; Chval, J.; Reiche, P. *Phys. Status Solidi* **1996**, *196*, K7.
(24) Esaks, T.; Kamata, M.; Saito. H. *Solid State Ionics* **1996**, *73*, 86.
(25) Takai, S.; Sugiura, K.; Esaka, T. *Mater. Res. Bull.* **1999**, *193*, 34.
(26) Blasse, G.; Brixner, L. H. *Chem. Phys. Lett.* **1990**, *409*, 173.
(27) Oishi, S.; Hirao, M. *Bull. Chem. Soc. Jpn.* **1990**, *63*, 984.
(28) Tanji, K.; Ishii, M.; Usuki, Y.; Hara, K.; Takano, H.; Senguttuvan, A. *J. Cryst. Growth* **1999**, *204*, 505.
(29) Fendler, J. H. *Chem. Rev.* **1987**, *87*, 877.
(30) Tanori, J.; Pileni, M. P. *Langmuir* **1997**, *13*, 639.
(31) Dixit, S. G.; Mahadeshwar, A. R.; Haram, S. K. *Colloids Surf., A.* **1998**, *133*, 69.
(32) Moulik, S. P.; Paul, B. K. *Adv. Colloid Interface Sci.* **1998**, *78*, 99.
(33) Ravey, J. C.; Buzier, M. J. *Colloid Interface Sci.* **1987**, *116*, 30.
(34) Sugimoto, T.; Khan, M. M.; Muramatsu, A. *Colloids Surf., A* **1993**, *70*, 167.
(35) Sugimoto, T.; Khan, M. M. Muramatsu, A.; Itoh, H. *Colloids Surf., A.* **1993**, *79*, 233.
(36) Shindo, D.; Park, G.-S.; Waseda, W.; Sugimoto, T. *J. Colloid Interface Sci.* **1994**, *168*, 478.
(37) Sugimoto, T.; Wang, Y. *J. Colloid Interface Sci.* **1998**. *207*, 137.
(38) Sasaki, N.; Murakami, Y.; Shindo, D.; Sugimoto, T. *J. Colloid Interface Sci.* **1999**, *213*, 121.
(39) Lee, S. M.; Cho. S. N.; Cheon, J. W. *Adv. Mater.* **2003**, *15(5)*, 441.
(40) Shi, C. S.; Wei Y. G.; Yang, X. Y.; Zhou, D. F.; Guo, C. X.; Liao, J. Y.; Tang, H. G. *Chem. Phys. Lett.* **2000**, *328*, 1.